

1 **Flow resistance of inertial debris flows**

2 Diego Berzi<sup>1</sup> and Enrico Larcán<sup>2</sup>

3 <sup>1</sup> Assistant professor, Dept. of Environmental, Hydraulic, Infrastructure, and Surveying Engineering, Politecnico di  
4 Milano, Milan, 20133, Italy. Email: diego.berzi@polimi.it

5 <sup>2</sup> Full professor, Dept. of Environmental, Hydraulic, Infrastructure, and Surveying Engineering, Politecnico di Milano,  
6 Milan, 20133, Italy. Email: enrico.larcan@polimi.it

7

8 **Abstract**

9 This work deals with the evaluation of the most suitable expression for the motion resistance of a  
10 debris flow. In particular, we focus on inertial debris flows, i.e., granular-fluid mixtures in which  
11 the particle inertia dominates both the fluid viscous force and turbulence; we provide, through an  
12 order of magnitude analysis, the criterion to be satisfied for a debris flow to be considered inertial  
13 and we show that most of real scale debris flows match this description. We then use the analytical  
14 relation between flow depth, depth-averaged velocity and tangent of the angle of inclination of the  
15 free surface recently obtained by Berzi and Jenkins in steady, uniform flow conditions to  
16 approximate the flow resistance in depth-averaged mathematical models of debris flows. We test  
17 that resistance formula against experimental results on the longitudinal profile of steady, fully  
18 saturated waves of water and gravel over both rigid and erodible beds, and against field  
19 measurements of real events. The notable agreement, especially in comparison with the results  
20 obtained using other resistance formulas for debris flows proposed in the literature, assesses the  
21 validity of the theory.

22

## 23 **Introduction**

24 Two-phase, depth-averaged mathematical models seem to be a useful tool to predict the propagation  
25 of a debris flow (Iverson 1997; Pitman and Le 2005), here defined as a dense (i.e., high  
26 concentrated) mixture of water and solid particles, driven down a slope by gravity. In this context,  
27 two different expressions for the depth-averaged resistances of the fluid and the particles should be  
28 provided. Also, the depth-averaged mathematical models should allow for the fluid and particle  
29 depths being different, as experimentally shown by Armanini et al. (2005) and Iverson et al. (2010).  
30 Different physical mechanisms contribute to the development of shear stresses, and therefore flow  
31 resistance, in particle-fluid mixtures: the fluid viscous force, the fluid turbulence, the inter-particle  
32 collisions and frictional contacts. The latter two are dominant in what we call ‘inertial debris flows’,  
33 which are the focus of the present paper. This is a wider definition with respect to the inertial  
34 regime described by Bagnold (1954), where only the inter-particle collisions were taken into  
35 account. On the other hand, we call ‘mudflows’ the debris flows dominated by the fluid viscous  
36 force. The fluid turbulence is negligible in the case of debris flows, because of the high particle  
37 concentration.

38 Recently, Berzi and Jenkins (2008a,b, 2009) have developed a two-phase theory to analytically  
39 describe the behavior of debris flows in steady, uniform and non-uniform flow conditions, when the  
40 degree of saturation (ratio of fluid to particle depth) is allowed to differ from unity; they  
41 successfully compared their analytical results with the experiments performed by Armanini et al.  
42 (2005) and Tubino and Lanzoni (1993) on the flows of water and different types of granular  
43 material (plastic cylinders, glass spheres and gravel). In particular, Berzi and Jenkins (2009)  
44 provided the expressions, further simplified by Berzi et al. (2010), for the resistance formulas of the  
45 two phases (fluid and particles), to be used in depth-averaged mathematical models.

46 Here, we provide a rational criterion, through an order of magnitude analysis, to define the  
47 aforementioned inertial debris flows. The order of magnitude analysis provides further justification

48 of the assumptions made by Berzi and Jenkins in developing their theory. Based on the description  
49 provided by Iverson (1997), we also show that most of real scale debris flows can actually be  
50 considered inertial. For sake of simplicity, we limit the analysis to fully saturated debris flows, i.e.,  
51 flows for which the particle and fluid depths above the either rigid or erodible bed (Armanini et al.  
52 2005) coincide. The order of magnitude analysis, though, holds in general for nearly saturated  
53 debris flows, i.e., flows for which the fluid and particle depths are slightly different. Limiting the  
54 analysis to fully saturated debris flows permits to compare the resistance formula obtained from the  
55 theory of Berzi and Jenkins with previous single-phase expressions suggested in the literature.  
56 Indeed, despite the rather trivial consideration that the expression of the flow resistance is crucial in  
57 mathematically modeling debris flows, a relatively small effort has been devoted to actually  
58 evaluate the reliability of the available resistance formulas. The few works on the topic (Hung  
59 1995; Naef et al. 2006) investigated the influence of the resistance formulas on problems dominated  
60 by acceleration and mass exchange phenomena, sometimes making use of real debris flow events as  
61 test cases. We claim, on the contrary, that a minimum requirement for a resistance formula is to  
62 predict the relation between flow depth, depth-averaged flow velocity and angle of inclination of  
63 the free surface observed in a well controlled environment, such as a laboratory, on simple flow  
64 configurations, such as steady, uniform, or non-uniform, flows.

65 The paper is organized as follows. In Section 2, we briefly summarize the governing equations for  
66 steady, uniform, and fully saturated debris flows and perform the order of magnitude analysis to  
67 identify inertial debris flows and support the theory of Berzi and Jenkins (2008a,b, 2009). Then, in  
68 Section 3, we introduce and discuss the most popular resistance formulas so far adopted in  
69 mathematical models of debris flows, and we test their capability to predict the longitudinal profile  
70 of steady, fully saturated waves of water and gravel over either rigid or erodible beds,  
71 experimentally measured by Iverson et al. (2010) and Tubino and Lanzoni (1993). For  
72 completeness, we also show comparisons between the predictions of the theory of Berzi and Jenkins  
73 and field measurements on inertial debris flows. Finally, we draw some conclusions in Section 4.

## 74 **Theory**

### 75 **Governing equations**

76 We let  $\rho$  denote the fluid mass density,  $c$  the particle concentration,  $g$  the gravitational acceleration,  
77  $\sigma$  the ratio of particle to fluid density,  $d$  the particle diameter,  $\eta$  the fluid viscosity,  $U$  the fluid  
78 velocity, and  $u$  the particle velocity. The particle Reynolds number  $R \equiv \rho d (gd)^{1/2} / \eta$  is defined in  
79 terms of these. In what follows, all quantities are made dimensionless using the particle diameter,  
80 the mass density of the particle material,  $\rho\sigma$ , and the gravitational acceleration. We take  $z = h$  to be  
81 the free surface, and  $z = 0$  to be the position of the bed of inclination  $\theta$ , parallel to the free surface.  
82 The flow configuration is depicted in Fig.1a.

83 In Table 1, we summarize the momentum balances and the constitutive relations reported by Berzi  
84 and Jenkins (2009) for the steady, uniform flow of fluid and particles over a bed, in presence of  
85 lateral confinement;  $s$ ,  $p$ ,  $S$  and  $D$  are the particle shear stress, the particle effective pressure (total  
86 particle pressure minus pore pressure), the fluid shear stress and the drag exerted by the fluid on the  
87 particles, respectively. There, and in what follows, a prime indicates a derivative with respect to  $z$ .  
88 The additional force exerted on the particles by the vertical sidewalls, separated by a gap of width  
89  $W$ , is taken into account on average through their coefficient of sliding friction,  $\mu_w$  (Berzi and  
90 Jenkins 2008a, b).

91 The expression for the drag is that suggested by Jenkins and Hanes (1998), where  $\delta = U - u$ , and  $3T$   
92 is the mean square of the particle velocity fluctuations,  $T$  being the granular temperature.

93 The adopted particle rheology is a linearization of the phenomenological rheology suggested by the  
94 French group G.D.R. MiDi (2004), with the particle stress ratio,  $s/p$ , that depends only on the so  
95 called inertial number,  $I \equiv u' / (p/c)^{1/2}$ . In the linear particle rheology reported on Table 1,  $\chi$  is a  
96 material coefficient of order unity and  $\check{\mu}$  is the tangent of the angle of repose of the dry granular  
97 material in absence of lateral confinement (Berzi et al. 2010). The linear particle rheology is

98 supposed to be valid at high particle concentrations (da Cruz et al. 2005). Actually, Jenkins (2007),  
 99 Jenkins and Berzi (2010) and Berzi and Jenkins (2011) showed that the phenomenological rheology  
 100 of the G.D.R. MiDi (2004) applies only in a region a few diameters far from the boundaries (i.e., the  
 101 free surface and the bed, in the present case), and provided the particle rheology in this core region  
 102 using a more fundamental approach based on kinetic theories of dense granular gases (Jenkins and  
 103 Savage 1983; Goldhirsch 2003; Jenkins 2006). The particle rheology of Table 1 applies, therefore,  
 104 to thick debris flows (particle depth greater than, say, ten diameters) characterized by a relatively  
 105 narrow range of particle stress ratios. Berzi and Jenkins (2009) showed that that narrow range of  $s/p$   
 106 corresponds, though, to a range of angles of inclination of the bed typical of both laboratory and  
 107 real scale debris flows; they also showed that the corresponding values of the particle concentration  
 108 are in the range 0.5 to 0.6, indicating that the flow is dense. This justifies the fact that  $c$  is taken  
 109 constant in the expressions of Table 1.

110 Finally, a mixing length approach is used to express the turbulent fluid shear stress in Table 1. Berzi  
 111 and Jenkins (2009) took into account the possibility that either a large-scale (with the mixing length,  
 112  $l$ , proportional to  $h$ ) or a small-scale turbulence (with  $l$  of the order of the mean distance between  
 113 the particles) develops in the region where both fluid and particles are present. According to many  
 114 authors (Bagnold 1954; Derksen 2008), though, the presence of the particles at high concentration  
 115 suppresses the large-scale turbulence. Thus, we take  $l$  to be roughly one tenth of a particle diameter.  
 116 Berzi and Jenkins (2009) used, as boundary conditions, the vanishing of the particle and fluid  
 117 stresses at the free surface. At the bed, instead, boundary conditions for the particle and fluid  
 118 velocity are required. For the latter, the no-slip condition seems to apply; previous works have  
 119 instead shown that the particles slip at a rigid bed (Richman 1988; Jenkins 2001), at least in absence  
 120 of interstitial fluid, with:

$$121 \quad u_0 \propto \frac{s_0}{p_0} \left( \frac{p_0}{c_0} \right)^{1/2}. \quad (1)$$

122 In Eq. (1), the sub-index indicates the location  $z$  at which a quantity is evaluated. In the case of  
123 erodible bed, instead, the no-slip condition applies also to the particles (Berzi and Jenkins 2008a,b).

124

### 125 **Order of magnitude analysis**

126 As already mentioned, the linear particle rheology applies to thick and dense granular flows; i.e.,  
127 flows characterized by  $h$  much greater than one and  $c$  of order unity; the particle specific mass and  
128 the tangent of the angle of inclination of the bed are both of order unity.

129 Given that the coordinate  $z$  is of order  $h$ , the particle momentum balance along  $z$  (Table 1) shows  
130 that  $p$  is of order  $h$ . The inertial number  $I$  is of order  $10^{-1}$ , according to physical and numerical  
131 experiments on simple shear flow of dry granular material (G.D.R. MiDi 2004) and recent theory  
132 (Berzi et al. 2011), at least when the particle stress ratio is not close to the yielding value  $\check{\mu}$ . Hence,  
133 from the definition of  $I$ , the shear rate  $u'$  is of order  $10^{-1}h^{1/2}$ . This implies that  $u$  is of order  $10^{-1}h^{3/2}$ ,  
134 also known as the Bagnold scaling (Mitarai and Nakanishi 2005); obviously, also the depth-  
135 averaged particle velocity,  $u_m$ , is of order  $10^{-1}h^{3/2}$ .

136 The granular temperature  $T$  scales with  $p$  (Jenkins 2007) and therefore is of order  $h$ . We now  
137 assume that the non-linear part of the drag coefficient in the expression of the drag force (Table 1)  
138 is entirely due to the particle velocity fluctuations, i.e.,  $\delta$  is negligible with respect to  $T^{1/2}$ . This  
139 implies that  $\delta$  is much less than  $h^{1/2}$  and, therefore, also much less than  $u$ . With this, the fluid and  
140 particle velocities would be approximately identical (single-phase approximation), and  $u' \approx U'$ , as  
141 assumed by Berzi and Jenkins (2008a,b, 2009); then,  $U$  is of order  $10^{-1}h^{3/2}$ . The constitutive  
142 expression for the fluid turbulent shear stress of Table 1 gives, therefore, that  $S$  is of order  $10^{-4}h$ ,  
143 with  $l$  of order  $10^{-1}$ . Thus,  $S'$  is of order  $10^{-4}$  and can be neglected with respect to the component of  
144 the fluid weight along  $x$  (first term on the right hand side of the fluid momentum balance in  
145 Table 1), which is of order unity; hence, the fluid momentum balance reduces to a balance between  
146 the component of the fluid weight in the flow direction and the drag (with the fluid turbulence

147 having no influence on the flow). The drag must therefore be of order unity. The expression of the  
 148 drag in Table 1 can then be used to obtain that  $\delta$  is of order  $h^{-1/2}$ , which is consistent with our initial  
 149 guess on  $\delta$ . If the depth  $h$  is not much greater than one, or if the inertial number is much smaller  
 150 than one, i.e., if the particle stress ratio is close to  $\bar{\mu}$ ,  $\delta$  cannot be neglected with respect to  $u$  and the  
 151 single-phase approximation no longer holds. The former can be the case for some laboratory debris  
 152 flows, as shown in Berzi and Jenkins (2008a, b), while the latter is certainly the case at the onset  
 153 and arrest of debris flows, whose modeling therefore require a full two-phase approach.  
 154 Eq. (1) shows also that  $u_0$  is of order  $h^{1/2}$  for flows over rigid beds, hence negligible with respect to  
 155  $u_m$  when  $h$  is much greater than one, given that the particle stress ratio,  $s/p$ , is of order unity (G.D.R.  
 156 MiDi 2004; Jop et al. 2005; Mitarai and Nakanishi 2007).  
 157 The conditions for the validity of the linear particle rheology (thick flow and high concentration)  
 158 permit therefore to ignore the difference in velocity between the fluid and the particles, at least far  
 159 from the onset and the arrest, the particle slip velocity at the rigid bed and the turbulent fluid shear  
 160 stress, as in Berzi et al. (2010).  
 161 Actually, the use of the linear particle rheology (Table 1) has not been justified, yet. That rheology  
 162 holds for dense and dry granular flows. The interstitial fluid affects the particle interactions at the  
 163 micro-mechanical level in a significant way if the Stokes number,  $St \equiv \sigma T^{1/2} R / 9$ , for the particles  
 164 is small (Joseph et al. 2001; Courrech du Pont et al. 2003; Berzi 2011). Hence, given that we have  
 165 shown that  $T^{1/2}$  is of order  $h^{1/2}$ , the influence of the interstitial fluid on the particle interactions can  
 166 actually be ignored, and the debris flow can be defined inertial, if  $St \approx 10^{-1} R h^{1/2}$  is much greater than  
 167 one, i.e., if  $R$  is much greater than  $10 h^{-1/2}$ . The typical flow depths of real scale debris flows are of  
 168 order one meter (Iverson 1997); with this, and using the definition of the Reynolds number, and the  
 169 values of density and viscosity appropriated for water, the aforementioned condition would imply  $d$   
 170 much greater than  $10^{-3}$  mm. It is worth mentioning that  $d = 0.1$  mm is the silt-sand boundary  
 171 (Iverson 1997).

172 According to Iverson (1997), 90% of particles in debris flows is composed of sand, gravel or larger  
 173 grains; the remaining 10% is composed of finer components, whose main effect is increasing the  
 174 apparent density and viscosity of the interstitial fluid, without changing though the order of  
 175 magnitude of  $\rho$  and  $\eta$  that we have employed in the present analysis (using the expressions reported  
 176 by Iverson,  $\rho$  and  $\eta$  would be about 1.2 and 1.4 times the corresponding values for clear water,  
 177 respectively). Hence, most of real scale debris flows are inertial and the theoretical solution to  
 178 steady, uniform flows reported by Berzi et al. (2010) applies to them.

179 We now derive, using the above analysis and the expressions of Table 1, the theoretical solution for  
 180 steady and uniform, fully saturated, inertial debris flows over rigid beds confined between vertical  
 181 sidewalls. With  $c$  approximately constant in the momentum balances of Table 1, the total shear  
 182 stress of the mixture and the particle pressure read

$$183 \quad s + S = \frac{\sigma c + 1 - c}{\sigma} (h - z) \sin \theta - \frac{\mu_w}{W} p (h - z), \quad (2)$$

184 and

$$185 \quad p = \frac{c(\sigma - 1)}{\sigma} (h - z) \cos \theta, \quad (3)$$

186 respectively. Given that the fluid turbulent shear stress is negligible in Eq. (2), the particle stress  
 187 ratio results linearly distributed,

$$188 \quad \frac{s}{p} = \frac{(\sigma - 1)c + 1}{(\sigma - 1)c} \tan \theta - \frac{\mu_w}{W} (h - z). \quad (4)$$

189 From the particle rheology of Table 1, also the inertial number is linearly distributed in the flow,

$$190 \quad I = \frac{1}{\chi} \left[ \frac{(\sigma - 1)c + 1}{(\sigma - 1)c} \tan \theta - \frac{\mu_w}{W} (h - z) - \check{\mu} \right]. \quad (5)$$

191 Using the definition of the inertial number and the particle pressure distribution (Eq. 3), we obtain,

$$192 \quad u' = \frac{1}{\chi} \left[ \frac{(\sigma - 1)c + 1}{(\sigma - 1)c} \tan \theta - \frac{\mu_w}{W} (h - z) - \check{\mu} \right] \left[ \frac{(\sigma - 1) \cos \theta}{\sigma} \right]^{1/2} (h - z)^{1/2}. \quad (6)$$



193 Eq. (6) can easily be integrated to obtain the velocity distribution along  $z$ , using the no-slip  
 194 boundary condition at the rigid bed (in accordance with the order of magnitude analysis),

$$195 \quad u = \frac{2}{3} \frac{1}{\chi} \left[ \frac{(\sigma-1)c+1}{(\sigma-1)c} \tan \theta - \check{\mu} \right] \left[ \frac{(\sigma-1) \cos \theta}{\sigma} \right]^{1/2} \left[ h^{3/2} - (h-z)^{3/2} \right] \\ - \frac{2}{5} \frac{1}{\chi} \frac{\mu_w}{W} \left[ \frac{(\sigma-1) \cos \theta}{\sigma} \right]^{1/2} \left[ h^{5/2} - (h-z)^{5/2} \right]. \quad (7)$$

196 Finally, integrating Eq. (7) between 0 and  $h$  allows to obtain the depth-averaged particle velocity, in  
 197 the case of mild slopes ( $\cos \theta \approx 1$ ),

$$198 \quad u_m = \frac{2}{5} \frac{1}{\chi} \left[ \frac{(\sigma-1)c+1}{(\sigma-1)c} \tan \theta - \check{\mu} \right] \left[ \frac{(\sigma-1) \cos \theta}{\sigma} \right]^{1/2} h^{3/2} - \frac{2}{7} \frac{1}{\chi} \frac{\mu_w}{W} \left[ \frac{(\sigma-1) \cos \theta}{\sigma} \right]^{1/2} h^{5/2}. \quad (8)$$

199 Eq. (8) can be inverted to obtain an expression for the so called friction slope,  $j$ , that, in uniform  
 200 flow conditions, equals  $\tan \theta$ :

$$201 \quad j = \frac{(\sigma-1)c}{(\sigma-1)c+1} \check{\mu} + \frac{5\chi}{2} \left[ \frac{\sigma(\sigma-1)}{(\sigma-1)c+1} \right]^{1/2} c \left[ \frac{u_m}{h^{3/2}} + \frac{2}{7} \frac{1}{\chi} \frac{(\sigma-1)^{1/2}}{\sigma^{1/2}} \frac{\mu_w}{W} h \right]. \quad (9)$$

202 It is customary to use the expression of the friction slope obtained in uniform flow conditions to  
 203 approximate the flow resistance in depth-averaged mathematical models of non-uniform flows  
 204 (Chow 1959). In this sense, Eq. (9) represents the resistance formula for saturated debris flows over  
 205 rigid beds in presence of lateral confinement obtained from the theory of Berzi and Jenkins  
 206 (2008a,b, 2009). The first term on the right hand side of Eq. (9) represents the minimum slope  
 207 (yield) for having a steady, uniform flow; as expected, it increases as the concentration increases.

208 We can obtain the resistance formula for saturated debris flows over erodible beds confined  
 209 between vertical sidewalls by assuming, as in Berzi and Jenkins (2008a), that the particle stress  
 210 ratio is at its yielding value at the bed. Eq. (4) therefore provides an additional relation to determine  
 211 the flow depth as a function of the slope,

$$212 \quad \check{\mu} = \frac{(\sigma-1)c+1}{(\sigma-1)c} \tan \theta - \frac{\mu_w}{W} h. \quad (10)$$

213 Using Eq. (10) in Eq. (8), and substituting  $j$  for  $\tan\theta$  gives

$$214 \quad j = \frac{(\sigma-1)c}{(\sigma-1)c+1} \tilde{\mu} + \frac{35\chi}{4} \frac{[\sigma(\sigma-1)]^{1/2} c}{(\sigma-1)c+1} \frac{u_m}{h^{3/2}}. \quad (11)$$

215 It is worth noticing that, in saturated flow conditions, the two-phase theory of Berzi and Jenkins  
216 reduces to a single-phase theory (the dimensional analysis has indeed shown that the fluid and the  
217 particle velocity are roughly identical, if the flow is thick). This will allow us to compare Eqs. (9)  
218 and (11) with the widely used, single-phase, resistance formulas mentioned in the next Section.

### 219 **Test of resistance formulas**

220 Unfortunately, it is quite difficult to make accurate measurements on granular flows, even in a well  
221 controlled environment such as a scientific laboratory. Usually, both the depth and velocity are  
222 optically measured through glassy sidewalls, thus influenced by the latter. Also, the determination  
223 of the depth is easy in the case of flows over rigid beds, while in the case of flows over erodible  
224 beds depends on the location of the bed itself, which is still under debate (Armanini et al. 2005;  
225 Jenkins and Berzi 2010; Berzi et al. 2010). We have shown in the previous section that the debris  
226 flow is not influenced by the boundaries, if the depth is much greater than, say, ten diameters. This  
227 condition is normally achieved in real scale events (Iverson 1997), while all of the available  
228 laboratory experiments on uniform debris flows over rigid beds are characterized by depths of  
229 roughly ten diameters (Armanini et al. 2005; Hotta and Miyamoto 2008). Experiments characterized  
230 by depths of over a hundred diameters are actually reported by Hotta and Miyamoto (2008), but  
231 they can be classified as mudflows ( $R$  is of order  $10h^{-1/2}$ ), not inertial debris flows. Finally, in the  
232 most general case, the depth and velocity of the particles differ from those of the fluid, and they  
233 should be measured separately.

234 To our knowledge, the only experimental campaign with detailed measurements of particle and  
235 fluid depths and depth-averaged velocities – calculated from the volume flow rates – and angle of

236 inclination of the free surface was performed by Armanini et al. (2005) on steady, uniform, debris  
237 flows over erodible beds; some experiments were also performed by Tubino and Lanzoni (1993),  
238 though, in that case, the difference between the fluid and particle depth was not measured. Berzi  
239 and Jenkins (2008a,b, 2009) have shown that their two-phase theory was able to predict in a notable  
240 way the experimental results of both Armanini et al. (2005) and Tubino and Lanzoni (1993).  
241 As already mentioned, a fair test of the performance of the theory of Berzi and Jenkins against other  
242 resistance formulas, based on single-phase approach, should be made using experiments on fully  
243 saturated debris flows. Unfortunately, those experiments are rather scarce. An alternative is to  
244 analyze steady, fully saturated waves translating along inclines at constant velocity (Fig.1b and 1c).  
245 Indeed, the equation describing the shape of a wave moving at constant velocity along a plane is  
246 (Pouliquen 1999b; Berzi and Jenkins 2009):

$$247 \quad \frac{dh}{dx} = \tan \theta - j. \quad (12)$$

248 We need an expression for the friction slope,  $j$ , – the boundary condition being the vanishing of  $h$  at  
249 a certain position  $x = L$  along the bed – to solve Eq. (12). Apart from the steady, uniform flows,  
250 this is therefore the simplest flow configuration that allows to assess the validity of a resistance  
251 formula.

252 A list of the most popular resistance formulas adopted so far in debris flow models is reported on  
253 Table 2. The Coulomb resistance formula (Savage and Hutter 1989; Iverson 1997; Pitman and Le  
254 2005) is commonly adopted in Earth Science related works; it is based on the assumption that the  
255 granular material slides over an incline as a solid object without internal shearing, with the constant  
256 basal friction angle,  $\phi$ , independent on the flow velocity and depth, in contrast with experimental  
257 evidence on both dry granular and debris flows (Pouliquen 1999a; Armanini et al. 2005). The  
258 Takahashi's (1991) formula has been quite successful in the Hydraulics literature on debris flows; it  
259 is based on the pioneering work on inertial granular flows of Bagnold (1954), who correctly  
260 described the physical mechanism at the origin of the particle pressure (the particle collisions), but

261 was wrong in assuming a Coulomb-like relation between the particle shear stress and pressure, as  
262 clearly proved by recent numerical simulations on simple shear flows (da Cruz et al. 2005). In the  
263 expression reported on Table 2,  $c^*$  is the concentration at the closest packing, taken to be 0.74 as for  
264 mono-dispersed spheres (Torquato 1995), while  $a$  is a parameter that takes into account the nature  
265 of the bed (rigid or erodible).

266 For completeness, we have also listed in Table 2 some resistance formulas that, although do not  
267 strictly apply to inertial debris flows, have nonetheless been suggested in the literature. As already  
268 mentioned, the resistance formulas based on the assumption that the fluid viscous force dominates  
269 over the particle inertia may apply to mudflows, not to inertial debris flows. Several rheologies have  
270 been proposed (e.g., Newtonian, Bingham, Herschel-Bulkley, Coulomb-viscous; see Naef et al.  
271 2006 for references and a more detailed discussion) to derive those ‘viscous’ resistance formulas. In  
272 Table 2, we report only the resistance formula based on the Newtonian laminar rheology, where

273  $R^* = R \left[ \left( c^* / c \right)^{1/3} - 1 \right]^{3/2} / 2.25$  is a modified particle Reynolds number that takes into account the  
274 influence of the concentration on the fluid viscosity, as suggested by Bagnold (1954).

275 On the opposite, there are some resistance formulas that emphasize the ‘turbulent’ behavior of  
276 debris flows (i.e., the Manning-Strickler and Voellmy formulas reported in Table 2; see, once again,  
277 Naef et al. 2006). We have already stated in the previous section that the fluid turbulence is likely to  
278 be suppressed when the concentration is high; turbulent-like formulas may therefore apply to the  
279 flow of fluid-particle mixture at low-moderate concentration, but, once again, not to inertial debris  
280 flows. In the expressions of Table 2,  $n$  and  $\xi$  are the dimensional Manning and Voellmy  
281 coefficients, respectively. In the Voellmy formula, a turbulent-like term is added to a yield term; for  
282 the latter, we adopt the expression derived by Berzi and Jenkins (2008a,b, 2009) (first term on the  
283 right hand side of Eq. 9).

284 Iverson et al. (2010) reported the aggregated results of 15 experiments, characterized by the same  
285 initial conditions, on debris flows of water and a mixture of gravel and sand over rigid, rough beds

286 (Fig.1b) in a rectangular channel of width,  $W$ , equal to 200 cm (200 diameters, given that the mean  
 287 diameter of the sediments was equal to 1 cm) and constant inclination  $\theta$  equal to  $31^\circ$ , in terms of  
 288 wave height as a function of time,  $t$ . After an initial acceleration, the velocity of the front of the  
 289 wave reached a value of about 10 m/s, i.e.,  $u_m = 32$  in dimensionless units, and remained roughly  
 290 constant for the most of the length of the channel. There, the wave is therefore approximately steady  
 291 in a frame of reference moving at constant velocity, with  $x = 32t$ . Fig.2 shows the comparisons  
 292 between the average results of the 15 experiments and those obtained by numerically solving  
 293 Eq. (12), with a fourth-order Runge-Kutta method, using the aforementioned six resistance formulas  
 294 for  $j$ ; i.e., Eq. (9) and the five expressions of Table 2. In the latter, we use:  $\sigma = 2.65$ , appropriated  
 295 for sand and/or gravel in water;  $\bar{\mu} = 0.5$ , the tangent of the angle of repose in a channel of infinite  
 296 width, obtained by Forterre and Pouliquen (2003) for dry sand (assuming that sand and gravel have  
 297 similar properties);  $c = 0.65$ , the average value of the concentration of sand near an erodible bed  
 298 measured by Pugh and Wilson (1999);  $\chi = 0.6$ , that allows to reproduce the experimental results on  
 299 debris flows of water and gravel in uniform flow conditions (Berzi et al. 2010);  $\tan\phi = 0.8$ , as  
 300 suggested by Iverson et al. (2010);  $a = 0.35$ , given that the bed is rigid (Takahashi 1991);  
 301  $n = 0.1 \text{ s/m}^{1/3}$ , as suggested by Rickenmann (1999);  $\xi = 1120 \text{ m/s}^2$ , as suggested by Buser and  
 302 Frutiger (1980), analyzing data on snow avalanches. Also, given that the channel width is about 20  
 303 times larger than the flow depth, we ignore the additional term due to the presence of sidewalls in  
 304 Eq. (9). The particle Reynolds number in the experiments of Iverson et al. (2010) is about 3100  
 305 (with  $\eta = 10^{-3} \text{ Pa}\cdot\text{s}$ ); given that  $h$  is of order ten diameters (Fig.2),  $R$  is much greater than  $10h^{-1/2}$   
 306 and the particle inertia dominates the flow. The roughness of the rigid bed helps to greatly reduce  
 307 the slip velocity of the particles, so that the conditions for the validity of the theory of Berzi and  
 308 Jenkins are probably satisfied, despite the fact that the flow is not really thick. The agreement  
 309 between the experimental and the theoretical wave profile obtained using Eq. (9) is notable in terms  
 310 of the maximum height reached by the wave; even more notable, if one keeps in mind that the

311 experimental data are characterized by a significant dispersion and that the theory was developed  
312 for a mono-dispersed mixture of particles and water. On the other hand the reproduction of the  
313 shape of the snout is less satisfactory. There the depth is less than ten diameters, so that the  
314 influence of the bottom boundary cannot be neglected: the rough bed acts as a source of energy to  
315 the flow (Richman 1988), and, as already mentioned, the validity of the local granular rheology of  
316 Table 1 is questionable. The use of the Coulomb formula in Eq. (12) leads to a linear profile; hence,  
317 the experimental tendency of the free surface to become parallel to the bed in the upwards direction  
318 cannot be reproduced, and apart from a region close to the snout, the flow depth is largely  
319 overestimated. The Takahashi and the Manning-Strickler formulas strongly overestimate the flow  
320 resistance, and therefore the wave height; the opposite for the Newtonian laminar formula. The  
321 results obtained with the Voellmy formula are the closest to the experiments, apart from those  
322 obtained with Eq. (9). Obviously, we could have improved the agreement between the experiments  
323 and the predictions obtained using the above mentioned empirical formulas, by tuning the  
324 parameters present in the different expressions (except for the Coulomb formula, whose unrealistic  
325 consequences on the wave profile are independent on the choice of  $\tan\phi$ ). The *a priori* choice of the  
326 parameters in the formulas, though, highlights the superiority of Eq. (9), that does not require an *ad*  
327 *hoc* parameter adjustment.

328 Tubino and Lanzoni (1993) reported measurements of the wave height as a function of time,  $t$ , for  
329 one of their experiments on debris flows of water and 3 mm gravel in a rectangular channel of  
330 width,  $W$ , equal to 20 cm (67 diameters). For that experiment, they also measured the velocity of the  
331 front, that they described as fully saturated, and found it constant and equal to 47.6 cm/s, i.e.,  
332  $u_m = 2.8$  in dimensionless units; once again, the flow can then be considered steady in a frame of  
333 reference moving at constant velocity, with  $x = 2.8t$ . Unlike the experiments of Iverson et al. (2010),  
334 the debris flow propagated over an erodible bed (Fig.1c), whose initial inclination,  $\theta_0$ , was equal to  
335  $17^\circ$ ; this ensures that a no-slip velocity applies at the interface with the bed, but introduces an

336 additional uncertainty in determining the position of the bed itself, represented by  $b$  in the sketch of  
337 Fig.1c. The local slope of the bed,  $\tan\theta$ , in Eq. (12), can be expressed as

338 
$$\tan \theta = \tan \theta_0 - \frac{db}{dx}, \quad (13)$$

339 and an additional equation is required to solve for the evolution of both  $h$  and  $b$  along  $x$ . Eq. (10)  
340 provides this additional relation.

341 Fig.3a,b show the comparisons between the experimental results of Tubino and Lanzoni (1993) and  
342 those obtained by numerically solving the system of Eqs.(10), (12) and (13), using again a fourth-  
343 order Runge-Kutta method, with Eq. (11) and the five resistance formulas of Table 2 for  $j$ , and the  
344 boundary conditions  $h = b = 0$  at  $x = L$ . We keep the same values for the parameters in the  
345 resistance formulas adopted in the case of Fig.2, but for the parameter  $a$  in the Takahashi's formula  
346 that, in the case of erodible bed, is supposed to be equal to 0.042 (Takahashi 1991). We take  $\mu_w$  in  
347 Eq. (10) to be equal to 0.39, as suggested by Berzi et al. (2010).

348 The particle Reynolds number  $R$  is about 500 and therefore much greater than  $10h^{-1/2}$  for the  
349 experiments of Tubino and Lanzoni (1993), given that  $h$  is of order ten diameters (Fig.3). The  
350 agreement between the experimental and the theoretical wave profile obtained using the theory of  
351 Berzi and Jenkins (Fig.3a) is remarkable. Also the shape of the snout is well reproduced in this case,  
352 despite the fact that the flow there is thin. This seems to suggest that the local granular rheology of  
353 Table 1 holds also in the proximity of the bottom boundary (erodible bed), if the latter acts as a sink  
354 of energy to the flow (Jenkins and Askari 1991). The use of Eq. (11) results also in an erodible bed  
355 which is substantially unperturbed by the wave propagation (Fig.3a). This is in accordance with the  
356 observations of Tubino and Lanzoni (1993), although they did not report direct measurements of the  
357 position of the bed. None of the other resistance formulas allows to reproduce the experiments; in  
358 particular, the Voellmy formula, that gives good results in the case of the experiments of Iverson et  
359 al. (2010), dramatically underestimates the resistances in this case (Fig.3b).

360 A final test of the theory would consist in evaluating its performance with regards to field data.  
361 Rickenmann (1999) compiled data sets of field and laboratory measurements of mean velocity, flow  
362 depth and angle of inclination of the bed from different literature sources. Assuming that the data  
363 refer to roughly uniform flows, i.e., flows for which the bed slope,  $\tan\theta$ , coincides with the friction  
364 slope,  $j$ , they can be used to assess the validity of the theory. In particular, we make comparisons  
365 with Eq. (9) neglecting the term associated with the frictional sidewalls, because the field data refer  
366 to natural channels with expected small ratio of flow depth to channel width. The condition of fully  
367 saturation is rather exceptional, though; as revealed by the experiments of Armanini et al. (2005),  
368 the flow is always over-saturated at mild slopes, i.e., the height of the water is greater than the  
369 height of the particles above the bed. Nonetheless, it can be shown that Eq. (9) is representative of  
370 the resistances also when the flow is over-saturated, if the concentration  $c$  is taken to be the bulk  
371 value over the entire flow depth (Berzi et al. 2010). Fig.4 shows the comparison between the field  
372 and laboratory measurements, reported by Rickenmann (1999), for which  $R$  is much greater than  
373  $10h^{-1/2}$ , and the theoretical predictions of Eq. (9), in terms of the ratio  $u_m/h^{3/2}$  against  $\tan\theta$ . The  
374 field measurements have been performed on the Torrente Moscardo in Italy (Arattano et al. 1996)  
375 and the Jiangia gully in China (Rickenmann, written comm., 2011); the laboratory measurements  
376 were performed by Wang and Zhang (1990), Garcia Aragon (1996) and Iverson and LaHusen  
377 (1993). The mean diameter of the granular material ranges between 1 mm and 1 cm. Given the  
378 usual values of the bulk concentration for debris flows (Takahashi 1991), we take  $c$  equal to 0.2 and  
379 0.6 in Eq. (9) to draw the two theoretical curves of Fig.4. The values of the other parameters in  
380 Eq. (9) are exactly the same used for the comparisons of Fig.2 and 3. Despite all the uncertainties  
381 that characterize the measurements, the most of the field and laboratory measurements are in the  
382 region between the two curves, and the trend of the  $u_m/h^{3/2}$  to increase with the bed slope is  
383 notably reproduced by the theory.



## 384 **Conclusions**

385 This work has focused on the resistance formulas to be used in mathematical models of inertial  
386 debris flows, i.e., granular-fluid mixtures for which both the fluid viscous forces and the fluid  
387 turbulence does not substantially affect the particle interactions at the micro-mechanical level. For  
388 simplicity, we have limited the analysis to fully saturated flows, i.e., flows for which the fluid and  
389 particle depths coincide.

390 The main results of the paper are: (i) the most of real scale debris flows (Iverson 1997) are inertial  
391 debris flows, given that the concentration is higher than 40%, so that the fluid turbulence is  
392 suppressed, and the particle Reynolds number is much greater than ten times the inverse of the  
393 square root of the non-dimensional flow depth, so that the fluid viscous forces are negligible with  
394 respect to the particle inertia; (ii) hence, there is no physical justification to adopt, in depth-  
395 averaged mathematical models of inertial debris flows, resistance formulas of either ‘viscous’, such  
396 as those based on Newtonian, Bingham or Herschel-Bulkley rheologies, or ‘turbulent’ origin, such  
397 as the Manning-Strickler or the Voellmy expression; (iii) the particle slip velocity at a rigid bed, i.e.,  
398 the influence of the bottom boundary, can be ignored only if the flow depth is much greater than ten  
399 diameters - this usually applies to real scale events, not to most of the available laboratory  
400 experiments on inertial debris flows; (iv) the physically based resistance formulas obtained from the  
401 theory of Berzi and Jenkins (2008a,b, 2009) allow to reproduce, in a notable way, both the  
402 experimental longitudinal profile of steady waves of water and gravel measured by Iverson et al.  
403 (2010) and Tubino and Lanzoni (1993), and the field measurements of real events reported in the  
404 literature and collected by Rickenmann (1999); (v) neither the Coulomb (Iverson 1997; Pitman and  
405 Le 2005) nor the Takahashi (1991) resistance formula allow to fit the experimental results, raising  
406 some doubts about their implementation in mathematical models of debris flows.

## 407 **Acknowledgements**

408 The authors are grateful to Prof. James Jenkins for his support and discussions related to this work.

## 409 **Notation**

410 *The following symbols are used in the paper:*

411

412  $a$  = coefficient in the Takahashi's formula [-];

413  $c$  = particle volume concentration [-];

414  $c_0$  = particle volume concentration at a rigid bed [-];

415  $c^*$  = particle volume concentration at the closest packing [-];

416  $d$  = particle diameter [m];

417  $D$  = drag force [-];

418  $g$  = gravitational acceleration [m/s<sup>2</sup>];

419  $h$  = particle depth over the bed [-];

420  $I$  = inertial number [-];

421  $j$  = friction slope [-];

422  $l$  = mixing length in the fluid turbulent shear stress [-];

423  $L$  = position of the wave front [-];

424  $n$  = Manning's coefficient [m<sup>1/3</sup>/s];

425  $p$  = particle pressure [-];

426  $p_0$  = particle pressure at a rigid bed [-];

427  $R$  = particle Reynolds number [-];

428  $R^*$  = modified particle Reynolds number [-];

429  $s$  = particle shear stress [-];

430  $s_0$  = particle shear stress at a rigid bed [-];

431  $S$  = fluid shear stress [-];

432  $St$  = Stokes number [-];

433  $t$  = time [-];

434  $T$  = granular temperature [-];

435  $u$  = particle velocity [-];

436  $u_0$  = particle slip velocity at a rigid bed [-];

437  $u_m$  = depth-averaged particle velocity [-];

438  $U$  = fluid velocity [-];

439  $W$  = channel width [-];

440  $x$  = coordinate in the flow direction [-];

441  $z$  = coordinate in the direction perpendicular to the flow [-];

442  $\chi$  = material coefficient [-];

443  $\delta$  = difference between the fluid and the particle velocity in the flow direction [-];

444  $\phi$  = Coulomb's basal friction angle [°];

445  $\eta$  = fluid viscosity [Pa·s];

446  $\bar{\mu}$  = yielding value of the particle stress ratio at the bed [-];

447  $\mu_w$  = wall friction coefficient [-];

448  $\theta$  = local angle of inclination of the bed [°];

449  $\theta_0$  = unperturbed angle of inclination of the erodible bed [°];

450  $\rho$  = fluid density [kg/m<sup>3</sup>];

451  $\sigma$  = ratio of particle density over fluid density [-];

452  $\xi$  = Voellmy's coefficient [m/s<sup>2</sup>].

## 453 **References**

- 454 Armanini, A., Capart, H., Fraccarollo, L., and Larcher, M. (2005). "Rheological stratification in experimental  
455 free-surface flows of granular-liquid mixtures." *J. Fluid Mech.*, 532, 269–319.
- 456 Arattano, M., Mortara, G., Deganutti, A.M., and Marchi, L. (1996). "Esperienze di monitoraggio delle  
457 collate detritiche nel torrente Moscardo (Alpi Carniche)" [experience from debris flow monitoring in the

458 Moscardo torrent], *Geoingegneria Ambientale e Mineraria*, 2-3, Supplemento: Quaderni di Studi no.20:  
459 Studi sui Debris Flow, 33-43 (in Italian).

460 Bagnold, R.A. (1954). "Experiments on a gravity-free dispersion of large solid spheres in a Newtonian fluid  
461 under shear." *Proc. R. Soc. Lond. A*, 225, 49–63.

462 Berzi, D. (2011). "Analytical solution of collisional sheet flows." *J. Hydraul. Eng.-ASCE*,  
463 doi:10.1061/(ASCE)HY.1943-7900.0000420.

464 Berzi, D., Di Prisco, C.G., and Vescovi, D. (2011). "Constitutive relations for steady, dense granular flows."  
465 *Phys. Rev. E*, 84, 031301.

466 Berzi D., and Jenkins, J.T. (2008a). "A theoretical analysis of free-surface flows of saturated granular-liquid  
467 mixtures." *J. Fluid Mech.*, 608, 393–410.

468 Berzi, D., and Jenkins, J.T. (2008b). "Approximate analytical solutions in a model for highly concentrated  
469 granular-fluid flows." *Phys. Rev. E*, 78, 011304.

470 Berzi, D., and Jenkins, J.T. (2009). "Steady inclined flows of granular-fluid mixtures." *J. Fluid Mech.*, 641,  
471 359–387.

472 Berzi, D., and Jenkins, J.T. (2011). "Surface Flows of Inelastic Spheres." *Phys. Fluids*, 23, 013303.

473 Berzi, D., Jenkins, J.T., and Larcher, M. (2010). "Debris Flows: Recent Advances in Experiments and  
474 Modeling." *Adv. Geophys.*, 52, 103–138.

475 Buser, O., and Frutiger, H. (1980). "Observed Maximum Run-out Distance of Snow Avalanches and The  
476 Determination of The Friction Coefficients  $\mu$  and  $\xi$ ." *J. Glaciol.*, 26(94), 121–130.

477 Chow, V.T. (1959). *Open-channel hydraulics*, McGraw-Hill, New York, NY.

478 Courrech du Pont, S., Gondret, P., Perrin, B., and Rabaud, M. (2003). "Granular avalanches in fluids." *Phys.*  
479 *Rev. Lett.*, 90(4), 044301.

480 da Cruz, F., Enman, S., Prochnow, M., Roux, J.-N., and Chevoir, F. (2005). "Rheophysics of dense granular  
481 materials: Discrete simulation of plane shear flows." *Phys. Rev. E*, 72, 021309.

482 Derksen, J. J. (2008). "Scalar mixing by granular particles." *AIChE J.*, 54(7), 1741–1747.

483 Forterre, Y., and Pouliquen, O. (2003). "Long-surface-wave instability in dense granular flows." *J. Fluid*  
484 *Mech.*, 486, 21–50.

485 Garcia Aragon, J. A. (1996). "A hydraulic shear stress model for rapid, highly concentrated flow." *J. Hydr.*  
486 *Res.*, 34, 589–596.

487 G.D.R. Midi (2004). "On dense granular flows." *Euro. Phys. J. E*, 14, 341–365.

488 Goldhirsch, I. (2003). "Rapid granular flows." *Ann. Rev. Fluid Mech.*, 35, 267–293.

489 Hotta, N., and Miyamoto, K. (2008). "Phase classification of laboratory debris flows over a rigid bed based  
490 on the relative flow depth and friction coefficients." *Int. J. Erosion Control Engin.*, 1(2), 54–61.

491 Hungr, O. (1995). "A model for the runout analysis of rapid flow slides, debris flows, and avalanches." *Can.*  
492 *Geotech. J.*, 32, 610–623.

493 Hungr, O. (2000). "Analysis of debris flow surges using the theory of uniformly progressive flow." *Earth*  
494 *Surf. Proc. Lndfrms.*, 25, 483–495.

495 Iverson, R.M. (1997). "The physics of debris flows." *Rev. Geophys.*, 35, 245–296.

496 Iverson, R.M., and LaHusen, R.G. (1993). "Friction in debris flows: inferences from large-scale flume  
497 experiments," in *Hydraulic Engineering '93*, edited by H. W. Shen, S. T. Su and Feng Wen, pp. 1604–  
498 1609, ASCE, New York.

499 Iverson, R.M., Logan, M., LaHusen, R.G., and Berti, M. (2010). "The perfect debris flow? Aggregated  
500 results from 28 large-scale experiments." *J. Geophys. Res.*, 115, F03005.

501 Jenkins, J.T. (2001). "Boundary conditions for collisional grain flows at bumpy, frictional walls," in  
502 *Granular Gases*, edited by T. Poschel and S. Luding, pp. 125–139, Springer, Berlin.

503 Jenkins, J.T. (2006). "Dense shearing flows of inelastic disks." *Phys. Fluids*, 18, 103307.

504 Jenkins, J.T. (2007). "Dense inclined flows of inelastic spheres." *Gran. Matt.*, 10, 47–52.

505 Jenkins, J.T., and Askari, E. (1991). "Boundary conditions for rapid granular flows: phase interfaces." *J.*  
506 *Fluid Mech.*, 223, 497–508.

507 Jenkins, J.T., and Berzi, D. (2010). "Dense Inclined Flows of Inelastic Spheres: Tests of an Extension of  
508 Kinetic Theory." *Gran. Matt.*, 12, 151–158.

509 Jenkins, J.T., and Hanes, D.M. (1998). "Collisional sheet flows of sediment driven by a turbulent fluid." *J.*  
510 *Fluid Mech.*, 370, 29–52.

511 Jenkins, J.T., and Savage, S.B. (1983). "A theory for the rapid flow of identical, smooth, nearly elastic  
512 particles." *J. Fluid Mech.*, 130, 187–202.

513 Jop, P., Forterre, Y., and Pouliquen, O. (2005). “Crucial role of sidewalls in granular surface flows:  
514 consequences for the rheology.” *J. Fluid Mech.*, 451, 167–192.

515 Joseph, G.G., Zenit, R., Hunt, M.L., and Rosenwinkel, A.M. (2001). “Particle-wall collisions in a viscous  
516 fluid.” *J. Fluid Mech.*, 433, 329–346.

517 Mitarai, N., and Nakanishi, H. (2005). “Bagnold scaling, density plateau, and kinetic theory analysis of dense  
518 granular flow.” *Phys. Rev. Lett.*, 94, 128001.

519 Mitarai, N., and Nakanishi, H. (2007). “Velocity correlations in dense granular shear flows: Effects on  
520 energy dissipation and normal stress.” *Phys. Rev. E*, 75, 031305.

521 Naef, D., Rickenmann, D., Rutschmann, P., and Mcardell, B.W. (2006). “Comparison of flow resistance  
522 relations for debris flows using a one-dimensional finite element simulation model.” *Nat. Hazard. Earth*  
523 *Sys.*, 6(1), 155–165.

524 Pitman, E.B., and Le, L. (2005). “A two-fluid model for avalanche and debris flows.” *Phil. Trans. R. Soc. A*,  
525 363, 1573–1601.

526 Pouliquen, O. (1999a). “Scaling laws in granular flows down rough inclined planes.” *Phys. Fluids*, 11, 542–  
527 548.

528 Pouliquen, O. (1999b). “On the shape of granular fronts down rough inclined planes.” *Phys. Fluids*, 11,  
529 1956–1958.

530 Pugh, F.J., and Wilson, K.C. (1999). “Velocity and Concentration Distributions in Sheet Flow above Plane  
531 Beds.” *J. Hydraul. Eng.-ASCE*, 125(2), 117–125.

532 Richman, M.W. (1988). “Boundary conditions based upon a modified Maxwellian velocity distribution for  
533 flows of identical, smooth, nearly elastic spheres.” *Acta Mech.*, 75, 227–240.

534 Rickenmann, D. (1999). “Empirical relationships for debris flows.” *Nat. Hazards*, 19(1), 47–77.

535 Savage, S.B., and Hutter, K. (1989). « The motion of a finite mass of granular material down a rough  
536 incline.” *J. Fluid Mech.*, 199, 177–215.

537 Takahashi, T. (1991). *Debris Flow*, Balkema, Rotterdam.

538 Torquato, S. (1995). “Nearest-neighbor statistics for packings of hard spheres and disks.” *Phys. Rev. E*, 51,  
539 3170–3182.

- 540 Tubino, M.A., and Lanzoni, S. (1993). "Rheology of debris flows: experimental observations and modeling  
541 problems." *Excerpta Ital. Contrib. Field Hydraul. Engng.*, 7, 201–236.
- 542 Wang, Z., and Zhang, X. (1990) "Initiation and laws of motion of debris flow." *Proc. Hydraulics/Hydrology*  
543 *of Arid Lands*, pp. 596–691, ASCE, New York.

## List of tables

**Table 1.** Momentum balances and constitutive relations for the steady, uniform, debris flow

Particle momentum balance along $x$	$s' = -c \sin \theta - D + 2 \frac{\mu_w}{W} p$
Particle momentum balance along $z$	$p' = -c(\sigma - 1) \cos \theta / \sigma$
Fluid momentum balance along $x$	$S' = -(1 - c) \sin \theta / \sigma + D$
Drag	$D \equiv \frac{c}{\sigma(1 - c)^{3.1}} \left[ \frac{3}{10} (\delta^2 + 3T)^{1/2} + \frac{18.3}{R} \right] \delta$
Particle rheology	$\frac{s}{p} = \check{\mu} + \chi I$
Fluid turbulent shear stress	$S = (1 - c) l^2 U'^2 / \sigma$

**Table 2.** Literature resistance formulas for debris flows

Resistance formula	$j$
Coulomb	$\tan \phi$
Takahashi	$\frac{25}{4} \frac{0.3a}{\left[ (c^*/c)^{1/3} - 1 \right]^2} \frac{\sigma}{\left[ (\sigma - 1)c + 1 \right]} \frac{u_m^2}{h^3}$
Newtonian laminar	$\frac{3}{R^* \left[ (\sigma - 1)c + 1 \right]} \frac{u_m}{h^2}$
Manning-Strickler	$\frac{n^2 g}{d^{1/3}} \frac{u_m^2}{h^{4/3}}$
Voellmy	$\frac{(\sigma - 1)c}{(\sigma - 1)c + 1} \check{\mu} + \frac{g}{\xi} \frac{u_m^2}{h}$



Figure1a  
[Click here to download high resolution image](#)

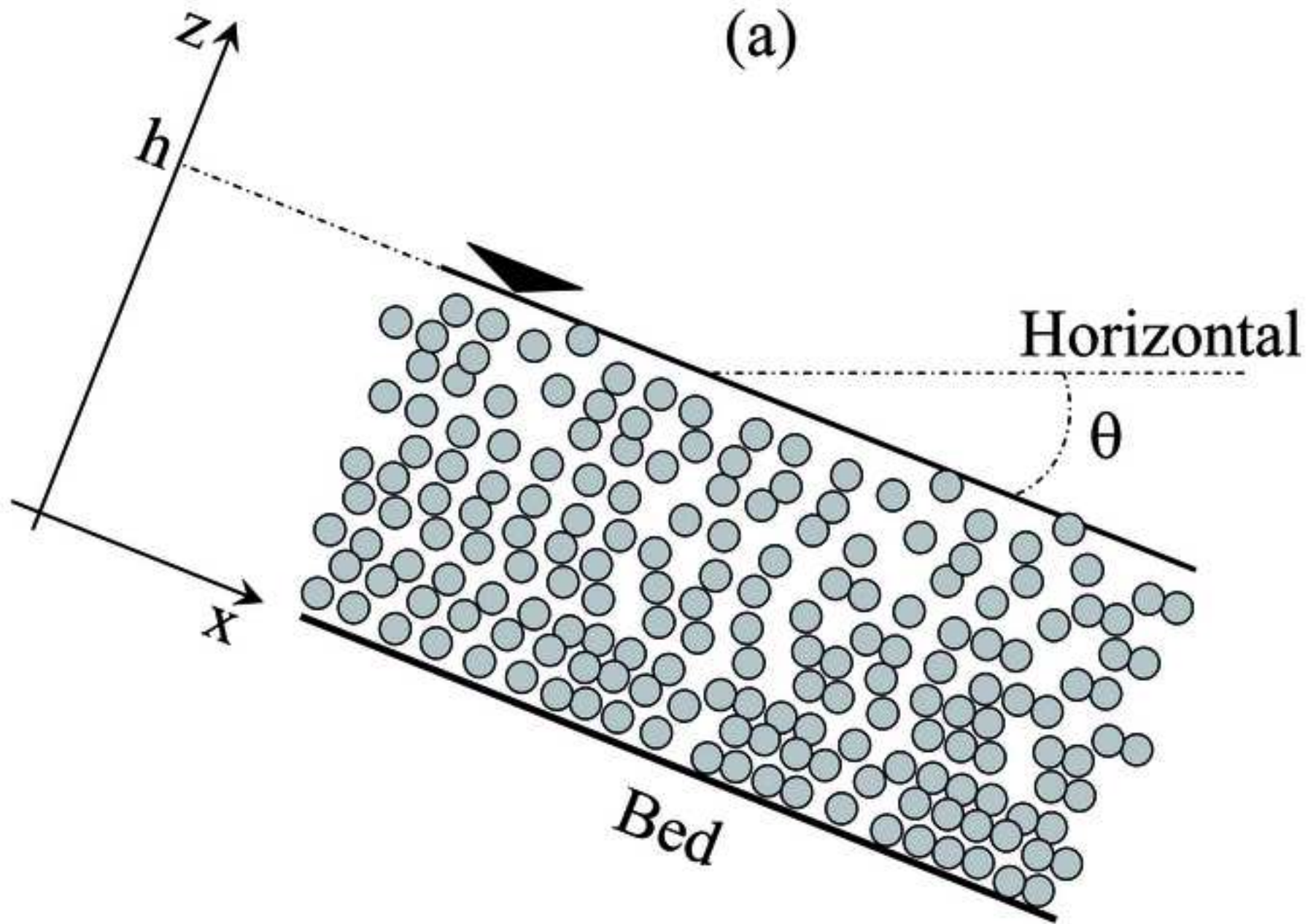


Figure 1b  
[Click here to download high resolution image](#)

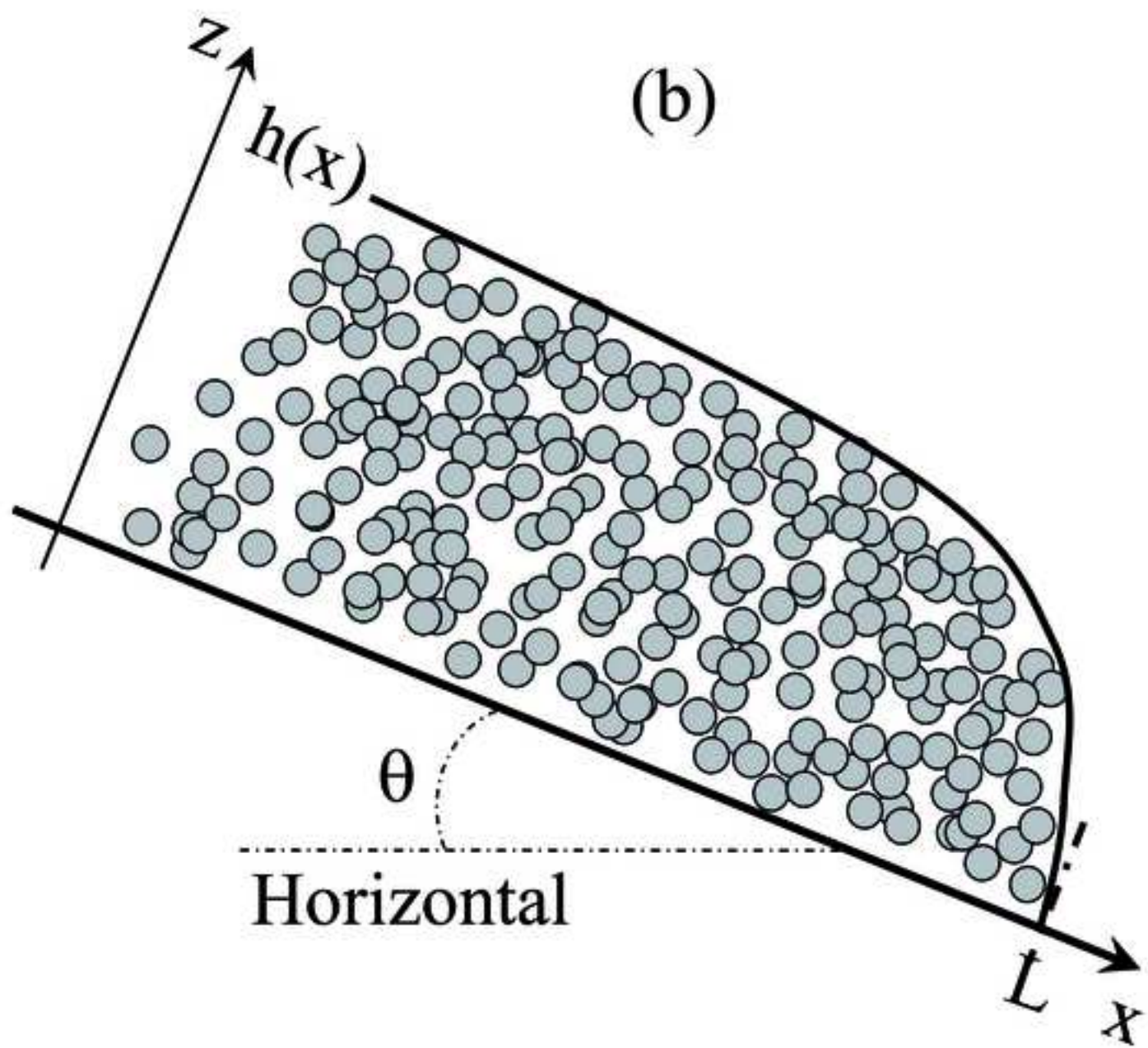


Figure 1c  
[Click here to download high resolution image](#)

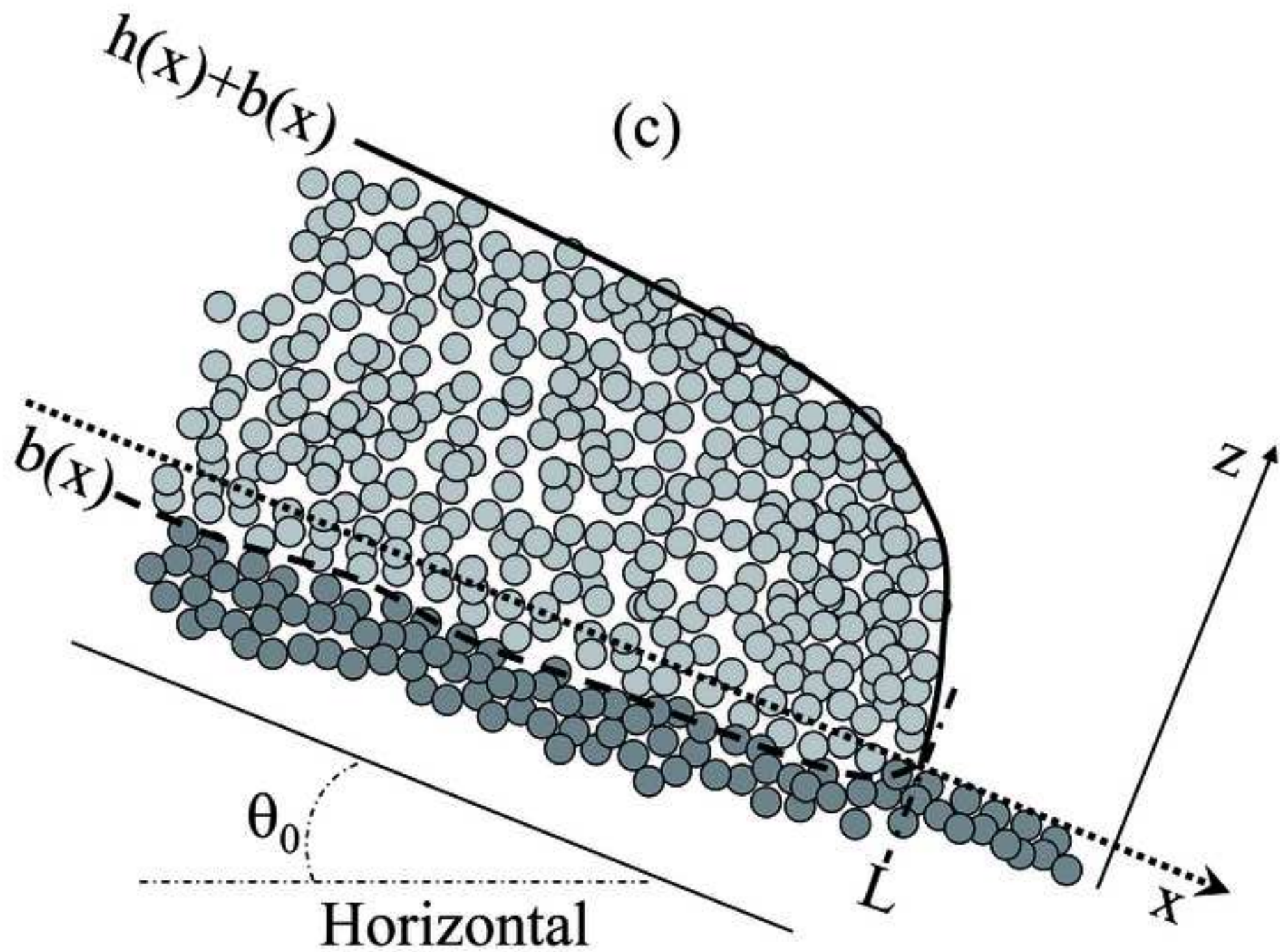


Figure2  
[Click here to download high resolution image](#)

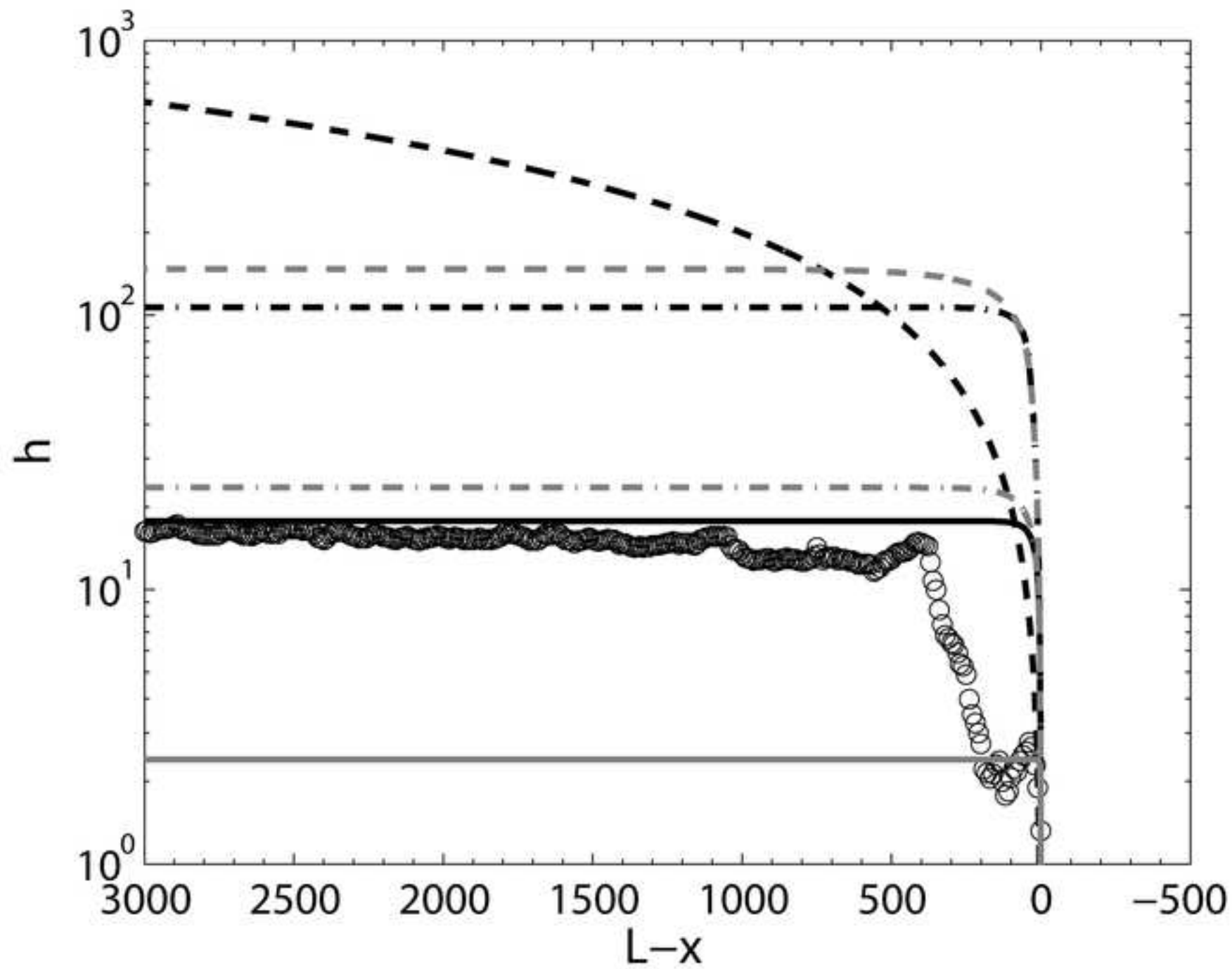
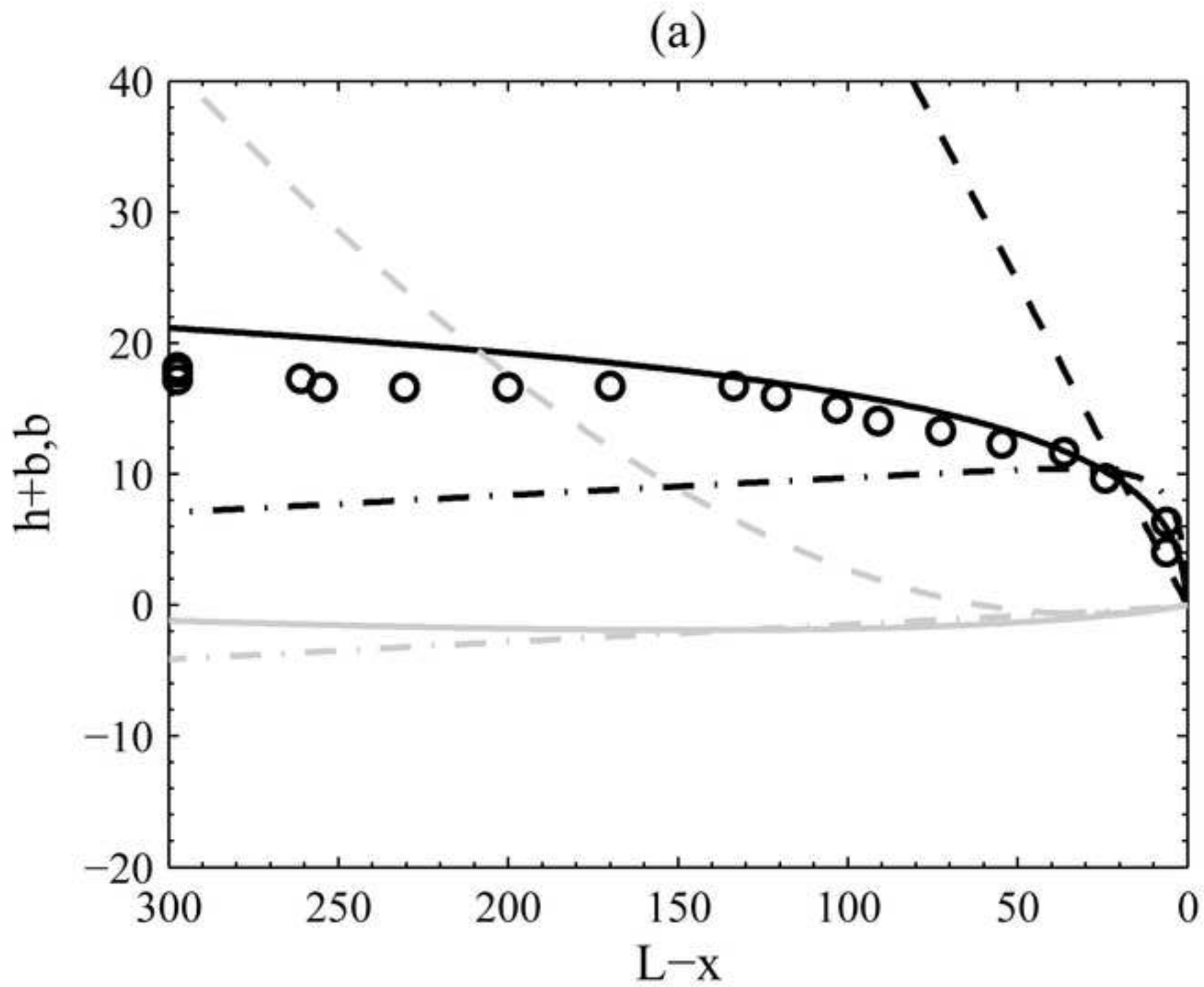


Figure3a  
[Click here to download high resolution image](#)



(b)

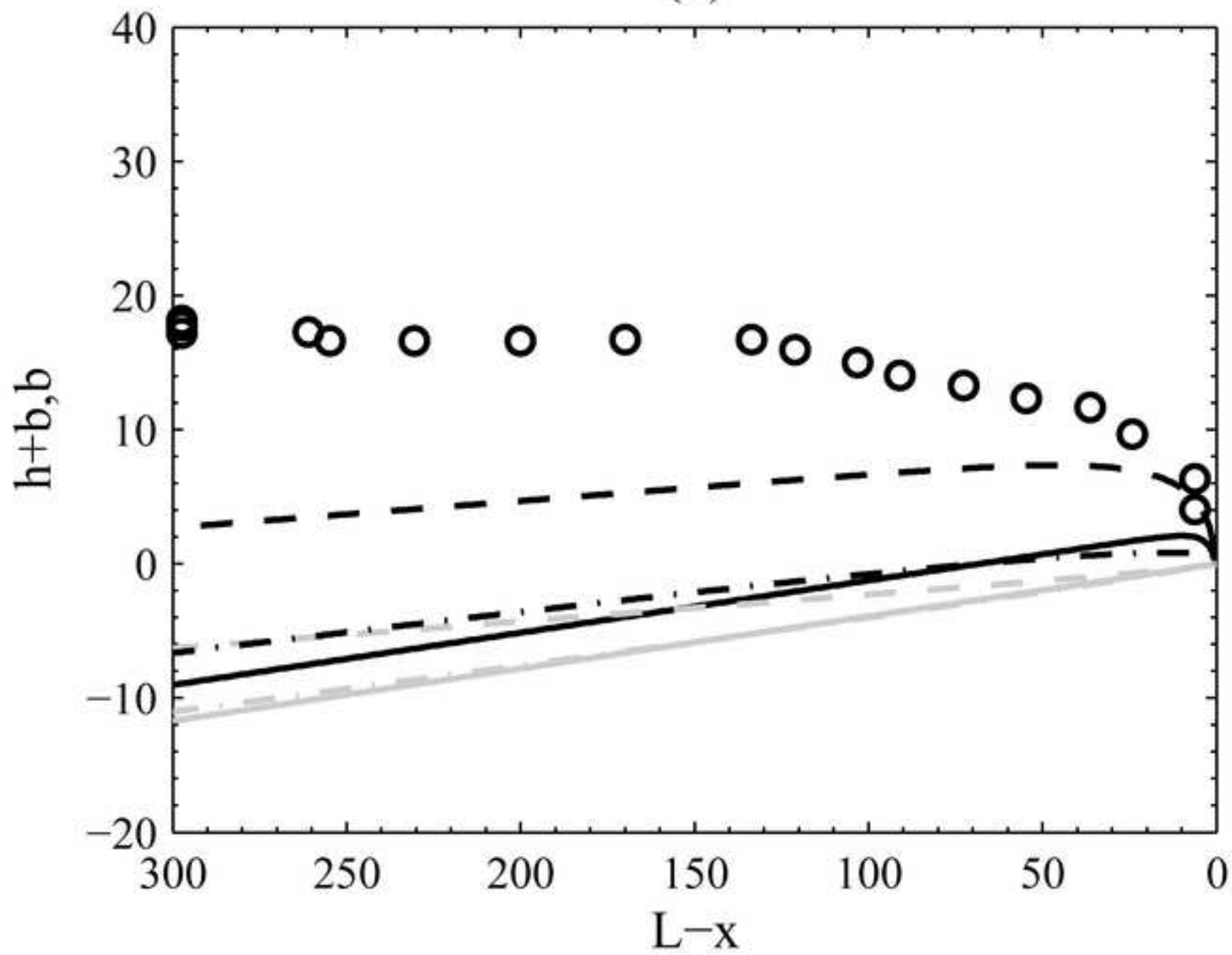
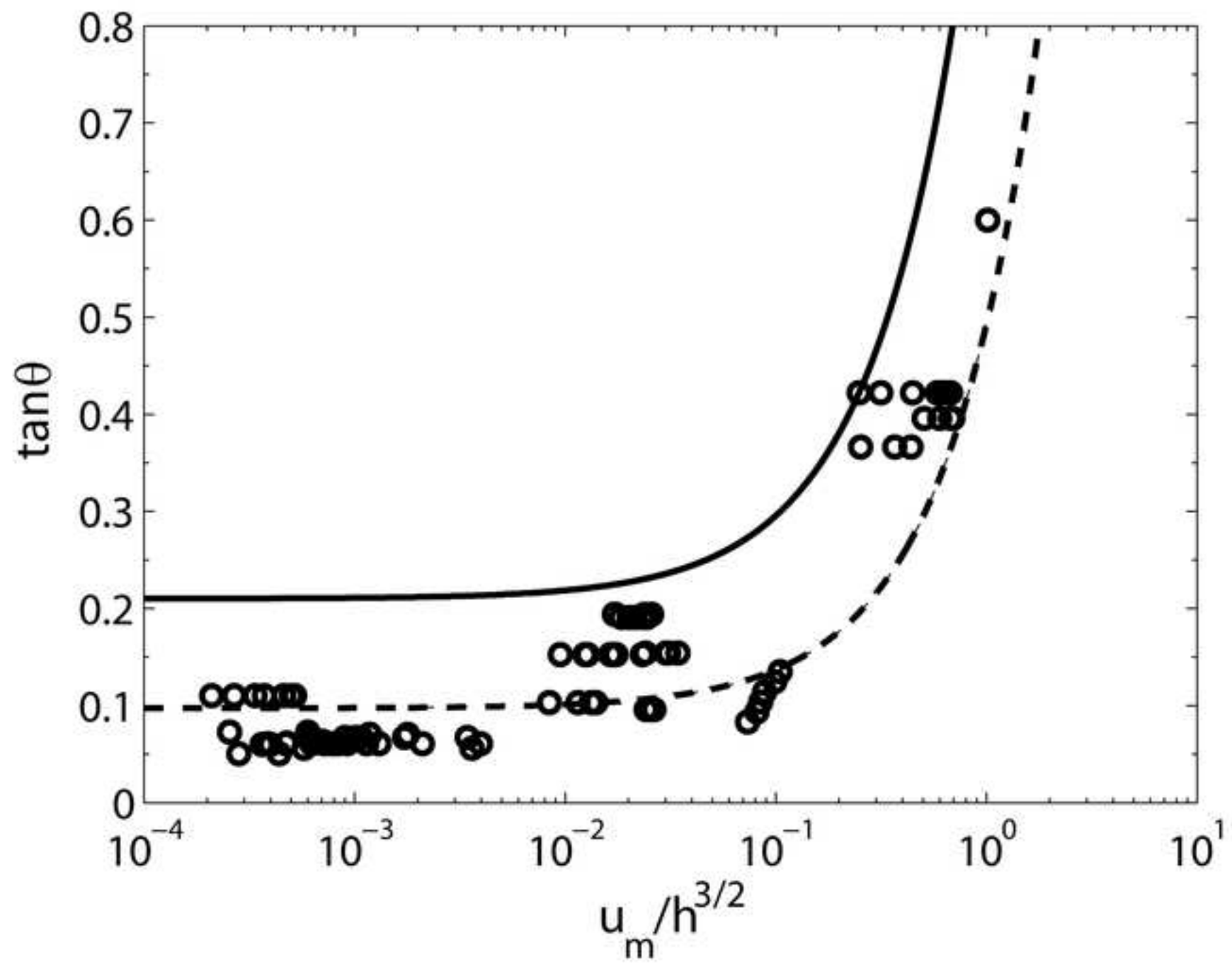


Figure4  
[Click here to download high resolution image](#)



## List of figure captions

**Figure 1.** (a) Steady, uniform, fully saturated debris flow. (b) Steady, non-uniform, fully saturated debris flow over a rigid bed. (c) Steady, non-uniform, fully saturated debris flow over an erodible bed.

**Figure 2.** Experimental (circles, from Iverson et al. 2010) against theoretical (lines) longitudinal profile of a steady wave over a rigid bed, obtained by solving Eq. (12) with the different expressions for  $j$ : Eq. (9) (solid black line); Coulomb (dashed black line); Takahashi (dot-dashed black line); Newtonian laminar (solid gray line); Manning-Strickler (dashed gray line); Voellmy (dot-dashed gray line).

**Figure 3.** (a) Experimental evolution of the free surface (circles, from Tubino and Lanzoni 1993) and theoretical evolution of the free surface (black lines) and the erodible bed (gray lines) for a steady wave over an erodible bed, obtained using: Eq. (11) (solid lines); Coulomb (dashed lines); Takahashi (dot-dashed lines). (b) Same as in Figure 3a, but using: Newtonian laminar (solid lines); Manning-Strickler (dashed lines); Voellmy (dot-dashed lines).

**Figure 4.** Field and laboratory measurements (circles, see the text for the sources) of the ratio  $u_m / h^{3/2}$  against bed slope for inertial debris flows. Also shown are the predictions of Eq. (9), for  $c = 0.6$  (solid line) and  $c = 0.2$  (dashed line).